E-ISSN: 2948-5231

Article

Journal of Asian Geography, 2026, Volume 5 (Issue 2), 1-17
https://doi.org/10.36777/jag2026.5.2.1

GIS-Based Modelling for Evaluating Soil Erosion Patterns in Ravine-Affected Regions of the Yamuna River, India

Robi Routh[1,*], Padmini Pani [2]

[1] Department of Geomorphology, Faculty of Geographical and Geological Sciences, Adam Mickiewicz University, Poznań, Poland 61-712.
[2] Centre for the Study of Regional Development, School of Social Sciences, Jawaharlal Nehru University, New Delhi, India 110067.

*Correspondence: robrou@amu.edu.pl

Received: 16 Apr 2026, Revised: 3 Aug 2026; Accepted: 26 Aug 2026; Published 29 Sep 2026

Abstract: Soil erosion poses a significant environmental challenge, particularly in ravine-affected areas where high-intensity rainfall can cause substantial soil loss, leading to declining soil fertility and the conversion of productive agricultural land into wasteland. This study estimates soil erosion rates in a severely ravine-affected area along the Yamuna River and examines temporal changes in erosion rates. The Revised Universal Soil Loss Equation (RUSLE) model was applied using various soil erosion parameters within the ArcGIS 10.5 platform. Multiple datasets, including rainfall and soil data, digital elevation models, and satellite imagery from Landsat to Sentinel-2, were used to derive the parameters required for soil erosion estimation. Soil erosion rates were assessed for six years: 1974, 1994, 2000, 2010, 2016, and 2020. The results indicated that soil erosion was highest in 1974 and lowest in 2020. Overall, soil erosion rates declined over the study period, except in 2000, when a slight increase was observed, possibly due to inadequate agricultural practices on levelled ravine lands. Ravine-land levelling emerged as an effective measure for reducing erosion; however, its long-term sustainability remains a major concern. Ravine and gully areas along the banks of the Yamuna River consistently exhibited relatively high soil erosion rates, although erosion rates varied over time. The results further indicated that increased vegetation cover was associated with reduced soil erosion rates in highly dissected ravine-affected areas. These findings may assist policymakers and local agricultural communities in developing more effective strategies for sustainable ravine-land management.

Keywords: Soil loss; Ravine Land; Land Levelling; RUSLE Model; Remote sensing; GIS; Yamuna River

1.0 Introduction

Soil is a complex natural resource composed of mineral, organic, water, and air components that interact to support terrestrial ecosystems. However, soil formation is a slow environmental process that requires considerable time, whereas soil erosion can occur at substantially higher rates (Lal, 2003; Montgomery, 2007). Accelerated soil erosion is a major environmental concern because it threatens land productivity, water quality, and ecosystem stability (Eslamian, 2014; FAO & ITPS, 2015; Huffman et al., 2013; Pimentel et al., 1995). Soil erosion is a physical process involving the detachment and downslope transport of soil particles driven by natural and anthropogenic factors (Nearing et al., 2017). Large quantities of soil are lost annually through various natural processes and human activities, resulting in widespread environmental degradation at the global scale (Borrelli et al., 2017; Huffman et al., 2013; Pak et al., 2008). In many landscapes, erosion rates exceed natural soil formation rates, thereby accelerating land degradation (Boardman, 2014). Ravine-affected areas represent particularly vulnerable landscapes because of their fragile and highly dissected topography (Manivannan et al., 2017) and susceptibility to severe erosion (Pani, 2016, 2018; Pani & Mohapatra, 2011; Sharma, 1982). The resulting loss of soil nutrients and fertility reduces land productivity and can ultimately transform productive agricultural land into wasteland, posing challenges to sustainable development and human well-being (Pani, 2018; Pani et al., 2022).

Soil erosion affects landscapes worldwide, with particularly severe impacts reported in many developing regions. According to the Global Assessment of Human-Induced Soil Degradation (GLASOD), approximately 1.96 billion hectares worldwide are affected by human-induced soil degradation (Borrelli et al., 2017; Oldeman, 2000; Sonderegger & Stephan, 2021). Of this area, approximately 1,094 million hectares are affected by water erosion, 548 million hectares by wind erosion, 240 million hectares by chemical degradation, and 83 million hectares by physical degradation (Oldeman, 2000). In India, soil erosion is particularly severe in several regions, especially during the monsoon season. Narayana and Babu (1983) estimated that approximately 5,334 million tonnes of soil are detached annually in India, of which approximately 2,052 million tonnes are transported as sediment yield. The Indian Institute of Remote Sensing has also estimated that approximately 147 million hectares of land in India are affected by soil erosion (Gupta, 2015). The widespread occurrence of soil erosion not only affects environmental quality but also has substantial implications for human well-being and land productivity (Ebrahimzadeh et al., 2018). Therefore, accurate estimation and spatial characterisation of soil erosion are essential for understanding its impacts and supporting effective land management.

Various approaches have been developed to assess soil erosion, ranging from field-based measurements to remote sensing and modelling techniques. Traditionally, soil erosion studies have relied on field-based measurements, which, although time-consuming and labour-intensive, provide essential ground-truth information for validating other assessment approaches. Advances in remote sensing and Geographic Information Systems (GIS) have subsequently enabled more efficient quantitative assessments and spatially explicit analysis across large areas (de Vente & Poesen, 2005; Morgan et al., 1998; Renschler & Harbor, 2002; Vrieling, 2006; Woodward, 1999). Remote sensing provides spatially extensive observations that can be acquired repeatedly over large areas, supporting the monitoring of land-surface conditions and changes over time (Vrieling, 2006). The integration of satellite imagery with GIS-based analysis has therefore facilitated the spatial assessment of soil erosion and its controlling factors. Based on these advances, numerous soil erosion models have been developed and are broadly classified into physical, conceptual, and empirical approaches (Eslamian, 2014). The Revised Universal Soil Loss Equation (RUSLE) is one of the most widely applied empirical models for estimating soil loss because of its relative simplicity, flexibility, and applicability across diverse environmental conditions (Ebrahimzadeh et al., 2018; Grauso et al., 2015; Renard et al., 1997). The RUSLE model has been applied across a range of landscapes, including plateaus, mountainous regions, forests, and badlands (Chuenchum et al., 2020; Kabanza et al., 2013; Pal, 2016; Rejani et al., 2016; Smith, 1999; van Rompaey et al., 2002), indicating its potential applicability to the rugged and highly dissected ravine landscapes of the Yamuna River basin.

Despite extensive research on soil erosion, important knowledge gaps remain regarding its long-term temporal variability, particularly in ravine landscapes. Previous studies have predominantly focused on short-term assessments or individual time periods, limiting understanding of long-term erosion trajectories. Moreover, soil erosion research has largely concentrated on agricultural lands, forests, river basins, and mountainous regions, while highly eroded ravine landscapes have received comparatively less attention. Although land-management

E-ISSN: 2948-5231
Article
Journal of Asian Geography, 2026, Volume 5 (Issue 2), 1-17
https://doi.org/10.36777/jag2026.5.2.1

interventions such as land levelling have been implemented to reduce erosion and facilitate agricultural reclamation, their long-term effectiveness and potential environmental consequences remain insufficiently understood. The role of vegetation cover in controlling erosion within highly incised ravine terrain also remains relatively understudied. Addressing these gaps, this study estimates historical soil erosion rates in the Yamuna River ravine system and examines their long-term temporal patterns and potential drivers. Specifically, this study aims to: (1) estimate soil erosion rates in severely ravine-affected areas; (2) analyse temporal changes in soil erosion from 1974 to 2020; and (3) assess the influence of land-use changes, particularly land levelling and vegetation cover, on erosion dynamics. By integrating RUSLE modelling with GIS and multi-temporal remote sensing datasets, this study provides a comprehensive assessment of long-term soil erosion dynamics and the potential influence of land-management and vegetation changes. The findings provide a scientific basis for understanding erosion dynamics and supporting more effective and sustainable soil and ravine-land management in erosion-prone regions.

2.0 Study Area

The research focuses on ravine-affected areas in selected districts of Uttar Pradesh along the Yamuna River. The Yamuna-Chambal ravine system is recognised as one of the most severely eroded ravine zones in India, extending across three major states: Uttar Pradesh, Madhya Pradesh, and Rajasthan. Each year, extensive areas of agricultural land within these ravine regions are transformed into wasteland as a result of severe soil erosion, thereby affecting the sustainable development of the region (Pani, 2016; Pani et al., 2022). The present study focuses on the ravine zone along the Yamuna River, covering parts of the Uttar Pradesh districts of Agra, Firozabad, Etawah, and Auraiya. Geographically, the study area extends from 26°29′25″ N to 27°18′34″ N latitude and 78°03′39″ E to 79°20′05″ E longitude. Physiographically, the region is characterised by generally flat to gently undulating topography (Figure 1). However, the specific ravine-affected terrain selected for this study is more rugged, with elevations ranging from 26 to 136 m. The study area falls within a semi-arid climatic zone. The region is densely populated, and the local population is largely dependent on subsistence agriculture for its livelihood.

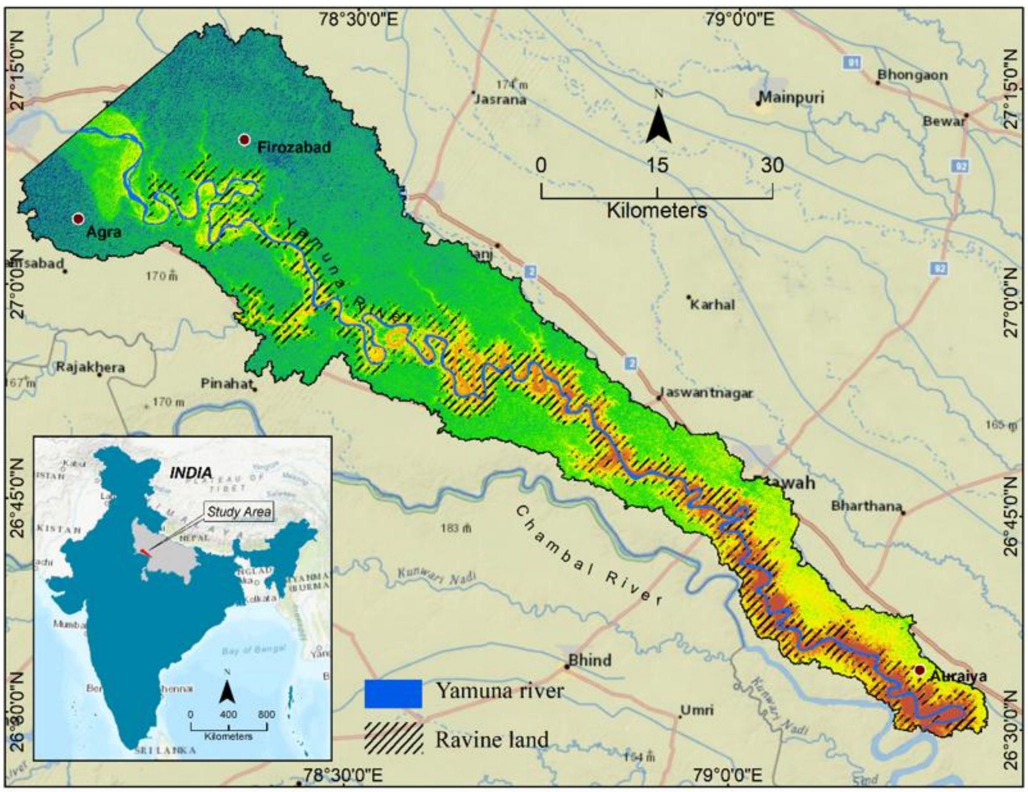

Figure 1: Location of the study area

3.0 Materials and Methodology

3.1 Datasets

A variety of quantitative datasets were used to derive and calculate the parameters required for the soil loss equation model. These datasets included rainfall data, a digital elevation model (DEM), soil texture data, and satellite imagery ranging from the Landsat series to the Sentinel-2 series. The selected years (1974, 1994, 2000, 2010, 2016, and 2020) were primarily determined by the availability of suitable satellite imagery covering the study area for land-cover mapping. Images with minimal cloud cover were selected to minimise cloud contamination within the study area. The 1974 Landsat MSS image was obtained as a Level-1 product, whereas the 1994, 2000, and 2010 Landsat images were obtained as Collection 2 Level-2 products. The 2016 and 2020 Sentinel-2 images were obtained as Level-2A products. As the Collection 2 Level-2 Landsat products and Sentinel-2 Level-2A products had already undergone atmospheric correction and geometric processing by the data providers, no additional preprocessing was performed before the analysis. A comprehensive list of the datasets used in this study is provided in Table 1.

Article
Journal of Asian Geography, 2026, Volume 5 (Issue 2), 1-17
https://doi.org/10.36777/jag2026.5.2.1
E-ISSN: 2948-5231

Table 1: Dataset used in soil erosion estimation

Soil Erosion Estimation Parameters	Types of Datasets	Source	Years	Spatial Resolution
Topographic Elevation	Cartosat DEM	Bhuvan Data Portal	2015	30 m
Rainfall Variation	IMD Monthly Rainfall Data	India- Water Resource Information System (WRIS)	1964 - 2020	Daily data
Soil Textural Information	Soil Texture Map	FAO Digital Soil Map	1974 - 2020	1:5,000,000
Land Use Land Cover	Landsat 1	USGS Earth Explorer	April 1974	80 m
	Landsat 5	USGS Earth Explorer	April 1994	30 m
	Landsat 5	USGS Earth Explorer	April 2000	30 m
	Landsat 5	USGS Earth Explorer	April 2010	30 m
	Sentinel-2A	Copernicus Open Access Hub	April 2016	10 m
	Sentinel-2B	Copernicus Open Access Hub	April 2020	10 m
Conservation Support	Numeric Data 0-1	Reference studies	-	-

3.2 Methodology

The Revised Universal Soil Loss Equation (RUSLE) model was employed to estimate soil erosion in the ravine-affected areas along the banks of the Yamuna River. The RUSLE model can be expressed as follows:

$$A = R \times K \times L \times S \times C \times P$$

where *A* represents the annual soil loss (t ha^{-1} year^{-1}), *R* represents rainfall-runoff erosivity, *K* represents soil erodibility, *L* represents the slope length factor, *S* represents the slope steepness factor, *C* represents the cover-management factor, and P represents the support-practice factor.

To run the RUSLE model, each parameter was derived from different datasets and calculated separately. All the raster layers (ranging from 10 to 80 m resolution) were resampled to a common 30 m spatial resolution using bilinear interpolation. The resulting layers were then multiplied using the Raster Calculation tool in ArcGIS 10.5.

3.2.1 Rainfall-Runoff Erosivity (R-factor)

Rainfall-runoff erosivity (R-factor) is a critical parameter in soil erosion modelling, as rainfall directly and indirectly affects soil erosion. High-intensity rainfall over long durations can result in significant soil erosion through surface runoff (Woodroffe & Jones, 2003). This rainfall-runoff relationship is quantified as the R-factor in soil erosion models (Lane et al., 1992; Wischmeier & Smith, 1978). Calculating the R-factor enables an understanding of the dynamics of surface runoff during rainfall events.

The R-factor can be calculated by multiplying the 30-minute interval rainfall intensity with the kinetic energy of the storm (Miheretu & Yimer, 2018). However, in the absence of rainfall intensity and storm kinetic energy for the study area, an empirical equation is employed to estimate the R-factor. Singh et al. (1981) formulated equations for estimating the R-factor under Indian conditions, incorporating both seasonal and annual rainfall variations, as shown in Eq. 1 and Eq. 2 (Vinay & Mahalingam, 2015).

$$R = 50 + 0.389 \times ASR(Average\ Seasonal\ Rainfall) \quad (1)$$

$$R = 79 + 0.363 \times AAR(Average\ Annual\ Rainfall) \quad (2)$$

A total of 56 years of IMD gridded monthly rainfall data were collected from the WRIS (Water Resource Information System) platform within the study area. Monthly rainfall data were categorized into six intervals: year 1964-1974, 1984-1994, 1990-2000, 2000-2010, 2006-2016, and 2010-2020, representing different time frames for analyzing soil erosion rates over distinct periods (Fig. 2). To calculate the R-factor for each study year, the annual average rainfall equation (Eq. 2), was utilized. Following Singh et al. (1981), the R-factor was expressed in metric erosivity units (MJ mm ha^{-1} h^{-1} year^{-1}).

3.2.2 Soil Erodibility (K-factor)

Soil erodibility, represented by the K-factor in the RUSLE model, refers to the susceptibility of surface topsoil to detachment by external forces (Renard et al., 1997). The K-factor is closely related to soil properties and is quantified numerically in the RUSLE model, with values typically ranging between 0 and 1 (Lane et al., 1992; Renard et al., 1997; Wischmeier & Smith, 1978). Higher values indicate a greater likelihood of soil erosion, while lower values suggest reduced susceptibility. According to the USLE equation, the value of the K-factor is usually taken from Wischmeier's Nomograph based on soil texture. Alternatively, it can be calculated using an empirical equation (Tosic et al., 2011). In the present study, the empirical equation formulated by Renard et al. (1997) was used to calculate the soil K-factor using Eq. 3:

$$K = \frac{2.1 \times 10^{-4} (12 - O_g)\, M^{1.14} + 3.25\,(S_r - 2) + 2.5\,(P_b - 3)}{100} \quad (3)$$

where K represents the soil erodibility, M represents the percentage of soil component (% sand, %silt, %clay), Og is the soil organic matter, Sr represents the structure codes of soil, which ranges from 1 to 4 (Table 2.1), and Pb represents the soil permeability code, ranges from 1 to 6 (Table 2.2).

The value of *M* is calculated as follows: M = (% sand + % silt)× (100 − % clay).

Journal of Asian Geography, 2026, Volume 5 (Issue 2), 1-17
https://doi.org/10.36777/jag2026.5.2.1
E-ISSN: 2948-5231

Table 2.1: Soil-structure codes adopted from Schwab et al. (1992), as cited in Chatterjee et al. (2014)

Structure Code	Soil structure	Soil particle diameter (in mm)
1	Very-fine-granular	Less than 1
2	Fine-granular	1-2
3	Mod-coarse granular	2-10
4	Blocky, platy, massive	More than 10

Table 2.2: Soil-permeability codes adopted from Schwab et al. (1992), as cited in Chatterjee et al. (2014)

Permeability Code	Permeability condition	Rate of permeability (in mm)
1	Rapid	More than 130
2	Mod-rapid	60-130
3	Moderate	20-60
4	Slow-moderate	5-20
5	Slow	1-5
6	Very slow	Less than 1

3.2.3 *Topographic Length and Steepness of Slope (LS-factor)*

Topographic length and slope steepness are represented by the LS-factor. Longer slope length and steeper slopes particularly when unobstructed by any conservation measure, increase runoff velocity, resulting in the transportation of a greater amount of sediment material (Wischmeier & Smith, 1978). Accurate value of the LS-factor helps to obtain a better estimation of soil erosion rates. Different authors have applied different methods to calculate the LS-factor in their respective studies, but there is still a lack of clarity regarding proper methodology and equations. Therefore, the study used a detailed methodology to calculate the LS-factor by applying the modified USLE equation proposed by Renard et al. (1997). This equation is particularly useful in areas related to highly dissected steep topography, barren land, and forest land (Chadli, 2016; Desmet & Govers, 1996). The equations for calculating the LS-factor in the study area are expressed as follows: Eqs. 4.1 - 4.4.

$$\boldsymbol{\alpha} = \frac{\mathrm{Sin(slope} \times 0.01745)/0.0896}{3 \times (\mathrm{sin(slope} \times 0.01745),\ 0.8) + 0.56} \tag{4.1}$$

$$\boldsymbol{\beta} = \frac{\alpha}{1+\alpha} \tag{4.2}$$

$$\mathbf{L} = \frac{\mathrm{power}((\mathrm{FlowAcc}+900),(\beta+1)) - \mathrm{power}\ (\mathrm{FlowAcc},(\beta+1))}{\mathrm{power}\ (30,(\beta+2)) \times \mathrm{power}(22.13,\beta)} \tag{4.3}$$

$$\mathbf{S} = \begin{cases} 10.8 \times \sin(\mathrm{slope} \times 0.01745) + 0.03, & \text{if } \tan\ (\mathrm{slope} \times 0.01745) < 0.09 \\ 16.8 \times \sin(\mathrm{slope} \times 0.01745) - 0.5, & \text{if } \tan\ (\mathrm{slope} \times 0.01745) > 0.09 \end{cases} \tag{4.4}$$

where *Slope* = terrain slope in degrees, derived from the 30 m Cartosat DEM. *FlowAcc* = flow accumulation (number of contributing cells), computed from the sink-filled DEM using ArcGIS Flow Accumulation tool. 900 represents the constant for slope-length adjustment in grid-based calculations (Desmet & Govers, 1996), 30 represents the grid-cell size (m), corresponding to the DEM spatial resolution, and 22.13 represents the length of the standard USLE plot (m).

The LS-factor of the study area was calculated by multiplying the values of L and S using the raster calculation tool in ArcGIS (LS = L × S).

3.2.4 *Surface Cover Management (C-factor)*

Surface cover management factor (C) in the RUSLE model quantifies how land use and vegetation management practices impact soil erosion rates (Renard et al., 1997). It represents the ratio of soil loss from clean tilled land to soil loss from agricultural cropland (Wischmeier & Smith, 1978). This vegetation cover management factor in the RUSLE model is expressed as a numerical value ranging from 0 to 1, where a value closer to 1 indicates the barren land, wasteland, or water bodies, while a value near 0 denotes dense vegetation cover (Lakkad & Shrivastava, 2016).

Most previous studies followed a traditional approach, in which C-factor values were often taken from the available literature. However, several other studies calculated the C-factor using the Normalized Difference Vegetation Index (NDVI; defined in Eq. 5) and an empirical equation.

Various equations have been developed for calculating the C-factor using the NDVI method. Van der Knijff (2000) formulated one such equation (Eq. 6), for calculating the C-factor. Similarly, Durigon et al. (2014) proposed another method for calculating the C-factor (Eq. 7) (Colman, 2018).

$$NDVI = (NIR - RED)/(NIR + RED) \tag{5}$$

$$Van\ der\ knijff, 2000\ Cf = exp\left\{-a\frac{NDVI}{b-NDVI}\right\} \tag{6}$$

$$Durigon, 2014\ Cf = 1.0\ \left(\frac{-NDVI+1}{2}\right) \tag{7}$$

Both Van der Knijff's (2000) and Durigon et al.'s (2014) equations have been widely used for calculating the C-factor worldwide. However, Van der Knijff's (2000) equation is more suitable for temperate climatic conditions, while Durigon et al.'s (2014) equation is more applicable in tropical climates under intensive rainfall (Almagro et al., 2019). Later on, Colman (2018) slightly modified Durigon's equation to correct systematic bias, as discussed by Almagro et al. (2019). Therefore, the modified Durigon et al. (2014) equation (Eq. 7) was adopted in the present study to derive the C-factor. NDVI was computed from both Sentinel-2 MSI and Landsat imagery (Table 1). All NDVI raster layers were resampled to a common 30 m spatial resolution using bilinear interpolation to match other RUSLE factor layers. Then C-factor values were calculated directly from the continuous NDVI raster layers by applying Eq. 7. This resulted in a continuous C-factor layer for each study year.

3.2.5 *Conservation Support and Practice (P-factor)*

Conservation support and practice factor (P) is another important parameter in the soil erosion estimation model. It represents the ratio between soil loss in topographic tillage slope and soil loss under conservation support conditions (Renard et al., 1997). The conservation support and practice factor (P) in the cultivated land includes contour farming, strip cropping, ridging, and terracing of the land (Roy, 2019). In the RUSLE model, the P-factor is expressed as a numerical value ranging from 0 to 1. A value of 0 indicates areas where perfect conservation practices have been implemented, including built-up land, plantation area, and contour cropping, whereas a value of 1 indicates the absence of any support practices (Ebrahimzadeh et al., 2018; Prasannakumar et al., 2012). In the present study, P-factor values for each land use class were obtained from the USLE reference handbook *Predicting Rainfall Erosion Losses: A Guide to Conservation Planning* (Wischmeier & Smith, 1978), along with other reference studies from similar physiographic regions (Table 3).

Table 3: P-factor values of different land use classes

Land use categories	P-factor value	Source
Waterbodies	0	(Wischmeier & Smith, 1978)
Sandbar	1	(Wischmeier & Smith, 1978)
Mixed forest	0.4	(Renard et al., 1997; Wischmeier & Smith, 1978)
Cropland	0.5	(Biswas & Pani, 2015)
Fallow land	0.9	(Pandey et al., 2007)
Ravine	1	(Benavidez et al., 2018; Renard et al., 1997)
Built-up land	0	(Wischmeier & Smith, 1978)

4.0 Results

4.1 *Spatial Distribution of Soil Erosion Parameters*

Each of the parameters used in soil erosion estimation was calculated using the datasets and equations described in the methodology section. The results for each of these parameters are discussed in the following subsections.

4.1.1 *Rainfall-Runoff Erosivity*

The Rainfall-Runoff Erosivity (R-factor) represents the erosive force of rainfall and its potential to cause soil erosion. It is a key input parameter in the RUSLE model. In this study, R-factors were calculated for six different years (1974, 1994, 2000, 2010, 2016, and 2020). To estimate the R-factor for each target year, rainfall data from the preceding ten years were used. For example, the R-factor for 1974 was derived using rainfall data from 1964 to 1974, and similarly for the remaining years. The R-factor value for each respective year is presented in Table 4.

The R-factor in the study area for the year 1974 ranged from 323.48 to 351.87 MJ mm ha^{-1} h^{-1} $year^{-1}$. Similarly, for the year 1994, the R-factor values ranged from 309.01 to 357.97 MJ mm ha^{-1} h^{-1} $year^{-1}$, followed by R-factor values ranging from 289.16 to 329.10 MJ mm ha^{-1} h^{-1} $year^{-1}$ in 2000. The R-factor values ranged from 248.86 to 300.31 MJ mm ha^{-1} h^{-1} $year^{-1}$ in 2010, values ranged from 255.39 to 294.23 MJ mm ha^{-1} h^{-1} $year^{-1}$ in 2016, and finally, for 2020, the R-factor varied from 244.90 to 302.09 MJ mm ha^{-1} h^{-1} $year^{-1}$, respectively (Table 4). The calculated R-factor values for the study area show a decreasing trend over time, corresponding to the decline in annual average rainfall across the decades (Figure 2; Table 4). In 1974, the R-factor ranged from 323.48 to 351.87 MJ mm ha^{-1} h^{-1} $year^{-1}$, with an average value of 338.36 MJ mm ha^{-1} h^{-1} $year^{-1}$. This was the highest among the study years and coincided with the highest recorded rainfall (714.48 mm on average). In contrast, the lowest R-factor was observed in 2010, averaging 266.20 MJ mm ha^{-1} h^{-1} $year^{-1}$, corresponding to a lower rainfall average of 515.69 mm. This consistent pattern indicates a close relationship between decreasing rainfall and lower erosivity values, highlighting how changes in climatic conditions directly influence soil erosion risk.

Table 4: Annual average rainfall (AAR in mm) and R-factor (in MJ mm ha^{-1} h^{-1} $year^{-1}$) in the study area over the years

Stations	AAR (1964-1974)	R-factor 1974	AAR (1984-1994)	R-factor 1994	AAR (1990-2000)	R-factor 2000	AAR (2000-2010)	R-factor 2010	AAR (2006-2016)	R-factor 2016	AAR (2010-2020)	R-factor 2020
Agra	695.10	331.3	633.61	309.01	673.81	323.59	480.20	253.31	560.46	282.45	614.58	302.09
Auraiya	737.62	346.8	768.51	357.97	604.53	298.44	504.99	262.31	486.47	255.59	457.03	244.9
Etawah	751.70	351.9	669.68	322.10	578.94	289.16	467.92	248.86	485.93	255.39	491.49	257.41
Firozabad	673.51	323.5	633.86	309.09	688.99	329.1	609.66	300.31	592.91	294.23	601.16	297.22
Average	714.48	338.36	676.42	324.54	636.57	310.07	515.69	266.20	531.44	271.91	541.07	275.41

E-ISSN: 2948-5231
Article
Journal of Asian Geography, 2026, Volume 5 (Issue 2), 1-17
https://doi.org/10.36777/jag2026.5.2.1

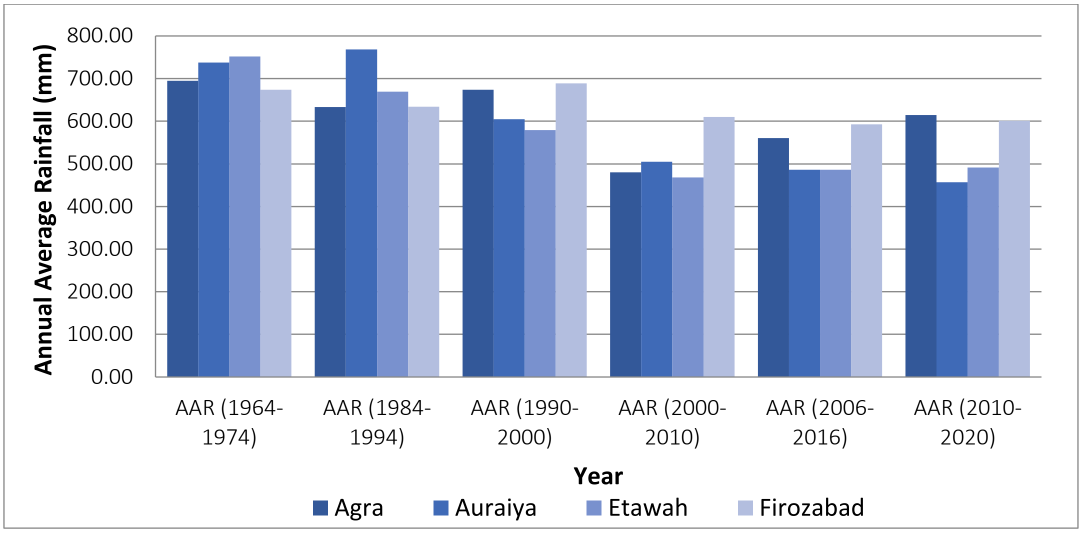

Figure 2: Annual average rainfall across six decadal intervals in the study area

4.1.2 Soil Erodibility

The soil erodibility factor (K) of the study area was calculated using an empirical equation, which integrates physical soil parameters. The results were obtained in both U.S. customary and SI units to ensure compatibility with previous studies and models. The study area comprised two main soil groups: Orthic luvisols and Eutric cambisols, with sandy-loam and loam textures, respectively. The calculated K-factor value of Orthic luvisols was 0.083 t h MJ^{-1} mm^{-1}, whereas that of Eutric cambisols was 0.058 t h MJ^{-1} mm^{-1} (Table 5). The maximum part of the study area is associated with loamy-textured soil, which influences soil stability and erosion potential. These values were derived using standard equations and are consistent with known ranges for these soil types.

Table 5: Soil erodibility (K-factor) of the study area in relation to soil properties

Soil classes	Soil texture	% of sand	% of silt	% of clay	Organic matter %	K-factor U.S. unit	K-factor SI unit
Orthic luvisols	Sandy loam	76	9.9	14.1	0.41	0.632	0.083
Eutric cambisols	Loam	36.4	37.2	26.4	1.07	0.439	0.058

4.1.3 Slope Length and Steepness

The slope length and steepness factor (LS) of the study area were calculated by using Eqs. 4.1 - 4.4. The LS-factor values in the study area range from 0.03 to 15.16. Most of the study areas exhibit lower LS-factor values, while higher values have a relatively limited spatial extent. Higher LS-factor values are typically associated with steep topographic slopes, especially in the ravine and gully lands along the banks of the Yamuna River (Figure 3a). These ravine lands are characterised by highly dissected terrain, with incision depths commonly ranging from approximately 30 to 40 m, and in several zones exceeding 60 m (R. S. Chatterjee et al., 2009; Pani, 2018; S. K. Verma et al., 2021). According to S. K. Verma et al. (2021), the Chambal ravines are very deep to extremely deep, with some areas reaching 30 - 60 m in depth. Similarly, Pani (2018) confirmed that deep ravines in the region exceed 30 m, while moderate ravines are typically around 15 m deep. Further, R. S. Chatterjee et al. (2009) classified very deep ravines in the Yamuna-Chambal belt as ranging from 60 to 80 m, emphasizing their role in extensive land degradation. As a result, these areas exhibit elevated LS-factor values due to their steep slopes and erosive potential (Figure 3b). This topographic configuration plays a major role in accelerating surface runoff and soil detachment.

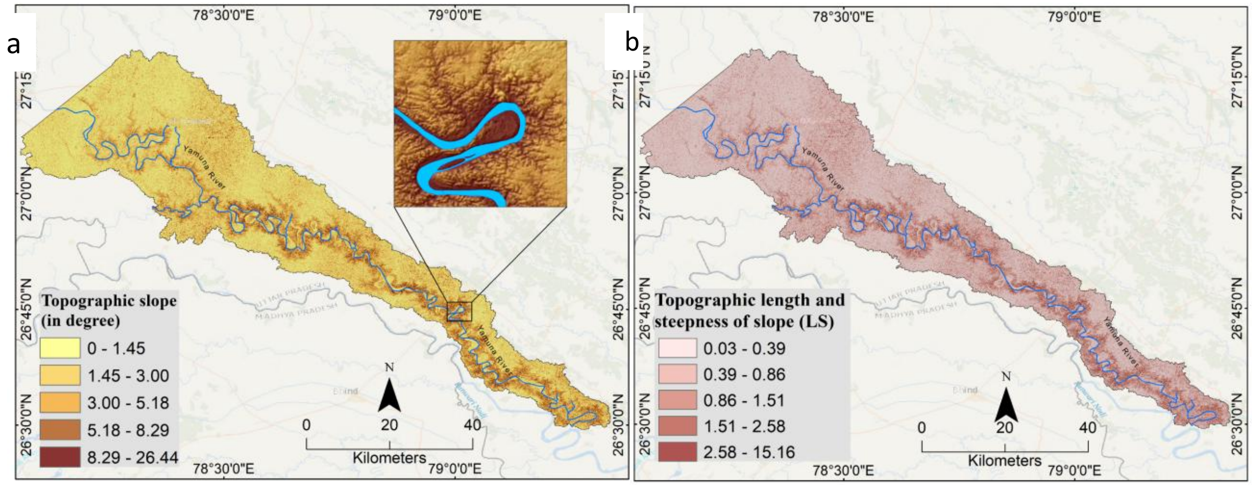

Figure 3: (a) Topographic slope in degrees; (b) topographic slope length and slope steepness (LS)

4.1.4 *Surface Cover Management and Conservation Support Practice*

The surface cover management factor (C) of the study area was derived from satellite imagery using NDVI (Normalized Difference Vegetation Index). The C-factor of the study area was calculated for six different years (Table 6). The results revealed an inverse relationship between NDVI values and C-factor values. Low values of NDVI correspond to areas with reservoirs, barren lands, and wastelands, while high NDVI values indicate areas with dense vegetation cover. However, in the C-factor map, a low value of C-factor signifies areas with vegetation cover, whereas high values of C-factor indicate reservoirs, fallow lands, and wastelands. Additionally, the conservation support and practice factor (P) of the study area was determined through a comprehensive land cover study, with values assigned based on established references listed in Table 3. These values reflect the varying degrees of land management interventions across the landscape.

Table 6: NDVI and corresponding C-factor values for the study area

Values	1974	1994	2000	2010	2016	2020
NDVI	- 0.633 to 0.781	- 0.177 to 0.54	- 0.469 to 0.392	- 0.274 to 0.533	- 0.316 to 0.691	- 0.358 to 0.873
C-factor Values	0.014 - 0.636	0.229 - 0.588	0.304 - 0.735	0.233 - 0.637	0.154 - 0.658	0.063 - 0.679

4.2 *The Annual Rate of Soil Erosion and Spatial Distribution*

The annual rate of soil erosion in the study area was estimated by multiplying all the parameters of the RUSLE model using the raster calculation tool in ArcGIS 10.5. Soil erosion rates were calculated for six different years to understand the changes in soil erosion dynamics over time. Table 7 presents the annual rate of soil erosion, ranging from 0 to 162.48 t ha^{-1} $year^{-1}$ in 1974. Similarly, the annual rate of soil erosion in 1994 ranged from 0 to 123.19 t ha^{-1} $year^{-1}$. Followed by soil erosion rate in 2000 was 0 to 149.89 t ha^{-1} $year^{-1}$. This represents a temporary increase in soil erosion compared to 1994, in the study area. The rate of soil erosion in 2010 ranged from 0 to 100.55 t ha^{-1} $year^{-1}$, in 2016 from 0 to 97.05 t ha^{-1} $year^{-1}$, and in 2020 the annual soil erosion rate was 0 to 85.2 t ha^{-1} $year^{-1}$, respectively. Among these six years, the highest rate of soil erosion was observed in 1974, while the lowest rate of soil erosion was recorded in 2020. The results indicate a gradual decline in soil erosion over the years, except for 2000, which showed a temporary increase in erosion, possibly due to unregulated agricultural or construction activities.

The rates of soil erosion were classified into five categories: Very low, Low, Moderate, High, and Very high. Approximately 80% of the study area experienced low to very low rates of soil erosion over the years, while only about 5% experienced high erosion rates (Table 8). The spatial distribution map (Figure 4) of the RUSLE model revealed that areas affected by ravine lands along the Yamuna River consistently showed high rates of soil erosion. These ravine lands, characterized by highly fragile and dissected terrain, exhibited high rates of erosion. As shown in Table 7, the rate of soil erosion tends to decrease over the years, except in 2000, when the rate increased slightly. After 2000, the erosion rate continued to decline, reaching its lowest point in 2020. This suggests a possible link between improved land use practices, vegetation growth, or conservation efforts during the last two decades.

Table 7: Annual rate of soil erosion in the study area over different years (t ha^{-1} $year^{-1}$)

Soil erosion classes	1974	1994	2000	2010	2016	2020
Very low	0 - 1.91	0 - 1.45	0 - 1.76	0 - 1.18	0 - 1.14	0 - 1
Low	1.92 - 6.37	1.46 - 4.83	1.77 - 5.88	1.19 - 3.94	1.15 - 3.81	1.01 - 3.01
Moderate	6.38 - 13.38	4.84 - 9.66	5.89 - 11.76	3.95 - 7.89	3.82 - 7.61	3.02 - 6.01
High	13.39 - 23.58	9.67 - 17.39	11.77 - 20.57	7.9 - 13.8	7.62 - 13.32	6.02 - 11.03
Very high	23.59 - 162.48	17.4 - 123.19	20.58 - 149.89	13.81 - 100.55	13.33 - 97.05	11.04 - 85.2

Article
Journal of Asian Geography, 2026, Volume 5 (Issue 2), 1-17
https://doi.org/10.36777/jag2026.5.2.1
E-ISSN: 2948-5231

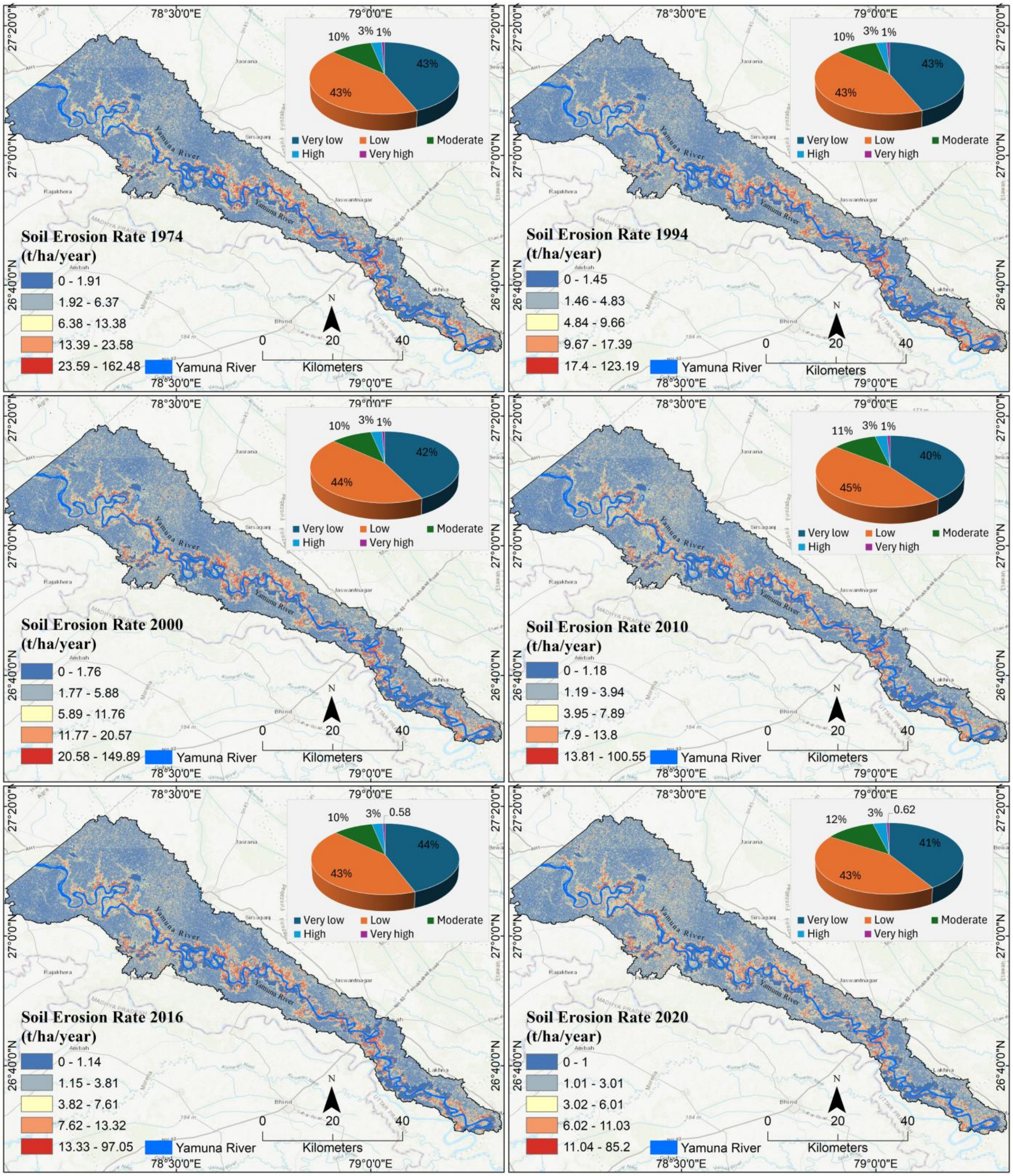

Figure 4: Annual rate of soil erosion in the study area over the years

E-ISSN: 2948-5231
Article
Journal of Asian Geography, 2026, Volume 5 (Issue 2), 1-17
https://doi.org/10.36777/jag2026.5.2.1

Table 8: Area (sq.km) and percentage of land under various soil erosion classes

Soil erosion classes	Area 1974	Area 1974 (%)	Area 1994	Area 1994 (%)	Area 2000	Area 2000 (%)	Area 2010	Area 2010 (%)	Area 2016	Area 2016 (%)	Area 2020	Area 2020 (%)
Very low	1111.61	43.61	1090.90	42.80	1094.95	42.97	1020.98	40.06	1125.40	44.15	1049.09	41.16
Low	1094.48	42.94	1104.76	43.34	1109.68	43.54	1158.40	45.46	1091.55	42.82	1088.95	42.72
Moderate	259.84	10.19	258.53	10.14	256.88	10.08	274.45	10.77	249.86	9.80	310.84	12.19
High	66.59	2.61	76.07	2.98	70.35	2.76	75.82	2.97	67.47	2.65	84.33	3.31
Very high	16.48	0.65	18.66	0.73	16.58	0.65	18.80	0.74	14.75	0.58	15.89	0.62
Total	2548.98	100	2548.93	100	2548.44	100	2548.46	100	2549.04	100	2549.11	100

5.0 Discussion

In the present study, the Revised Universal Soil Loss Equation (RUSLE) model has been utilized to understand soil erosion rates over the years in the study area. The result of the RUSLE model indicates that the ravine lands in the study area are characterized by high rates of soil erosion, although the rate of soil erosion has changed over the years. Changes in soil erosion rates were mostly associated with variations in rainfall and changes in land management practices, such as ravine land transformations and increasing vegetation cover. The research attempted to elucidate the role of ravine land and vegetation cover on soil erosion rates in the study area.

5.1 Role of Ravine-Land Transformation in Soil Erosion

Ravine-land transformation was found to play an important role in soil erosion dynamics. Ravine land transformations, such as land levelling and ravine land reclamation, significantly influence erosion rates (Hajgh, 1984; Marzolff & Pani, 2018; Pani, 2016, 2018, 2020; Tagore et al., 2021). Field observations revealed extensive areas of land levelling in the study area (Plate 1). Ravine lands are highly dissected and ineffective for human activity (Nadal-Romero & Regüés, 2010; Ranga et al., 2016); therefore, these undulating ravine lands in the study area have been levelled over time. Heavy machinery and earth tillage machines were used to level these lands, which were then utilized for various primary and secondary activities such as farming and construction works (Marzolff & Pani, 2018; Pani, 2020; Sikka et al., 2018) (Figure 5a). Consequently, the transformation of the ravine land and its use for different activities have led to a significant reduction in soil erosion rates over the years. The declining trend in annual soil erosion rates across the study period (Table 7) reflects the significant influence of land management interventions. One of the primary drivers has been land levelling, which transformed undulating terrain into cultivable land. The area of ravine land progressively decreased from 434.78 sq.km in 1974 to 177.07 sq.km in 2020, as shown in Table 9, resulting in a corresponding reduction in erosion rates. This is further supported by a scatter plot in Figure 6, which shows a positive relationship between ravine-land area and soil erosion rate, indicating that larger areas of ravine land are generally associated with higher erosion rates. The studies further observed that most land levelling associated along the edges of the ravines, where the terrain is characterised by shallow ravines (< 5 m deep). In contrast, the interior parts adjacent to the ravine consist of deeper ravines, typically > 30 m deep, with V-shaped, while the moderate ravines typically 5 - 30 m deep, with U-shaped (Figure 5b). These inner zones are often challenging to reclaim due to inaccessibility.

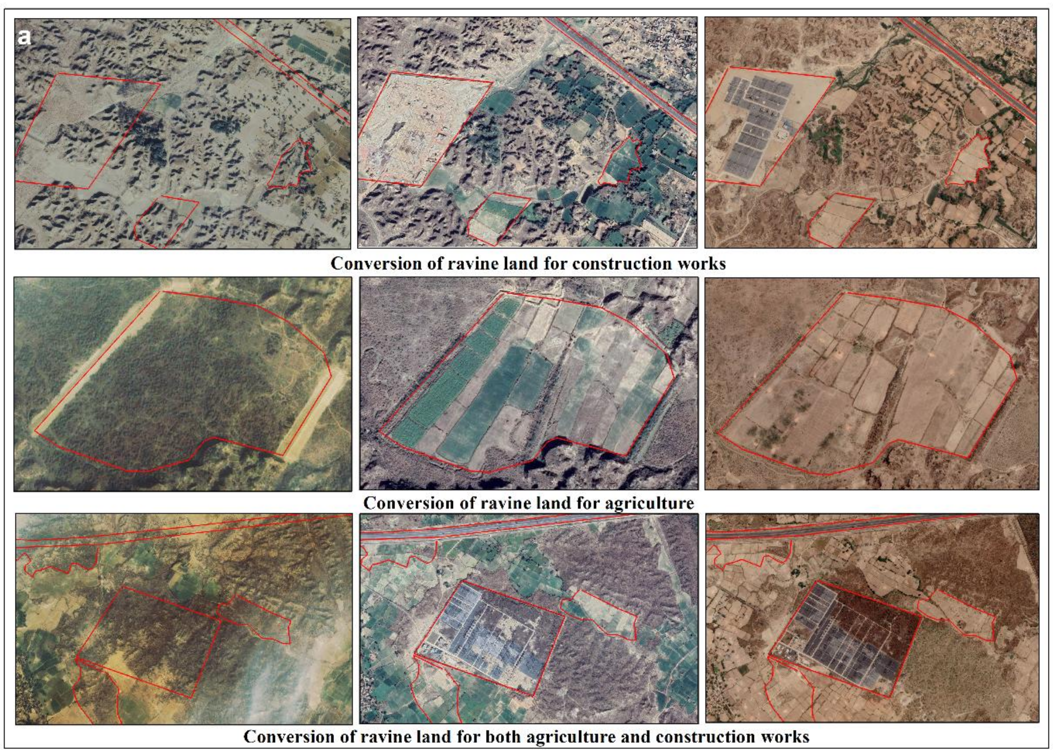

E-ISSN: 2948-5231
Article Journal of Asian Geography, 2026, Volume 5 (Issue 2), 1-17
https://doi.org/10.36777/jag2026.5.2.1

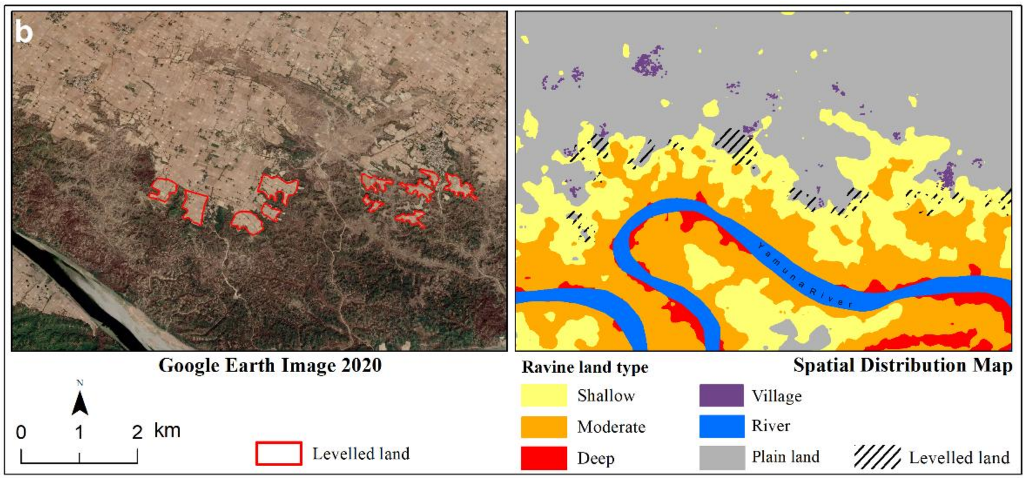

Figure 5: (a) Ravine land levelling and conversion of ravine land for farming and construction; (b) types and spatial distribution of ravine land along the Yamuna River

At the same time, the study highlighted the critical importance of continuous maintenance of levelled lands. These areas require regular refilling after each rainy season and sustained agricultural practices; otherwise, the surface may begin to form small rills and gullies during rainfall events, eventually reverting to wasteland (Pani, 2018; Pani & Mohapatra, 2011). This was evident in the year 2000, when due to lack of agricultural activities in levelled land, some portions of levelled land formed into gullies and converted levelled land back to wasteland, thereby increasing the area of ravine land again in 2000 (**Table 9)**, and as a result increases in soil erosion rate in 2000 (**Table 7**; **Fig. 7).** This highlights that, while land levelling plays a significant role in reducing soil erosion rates, proper utilization and continuous maintenance of levelled ravine land are essential to effectively prevent soil erosion and sustain the land productivity over time.

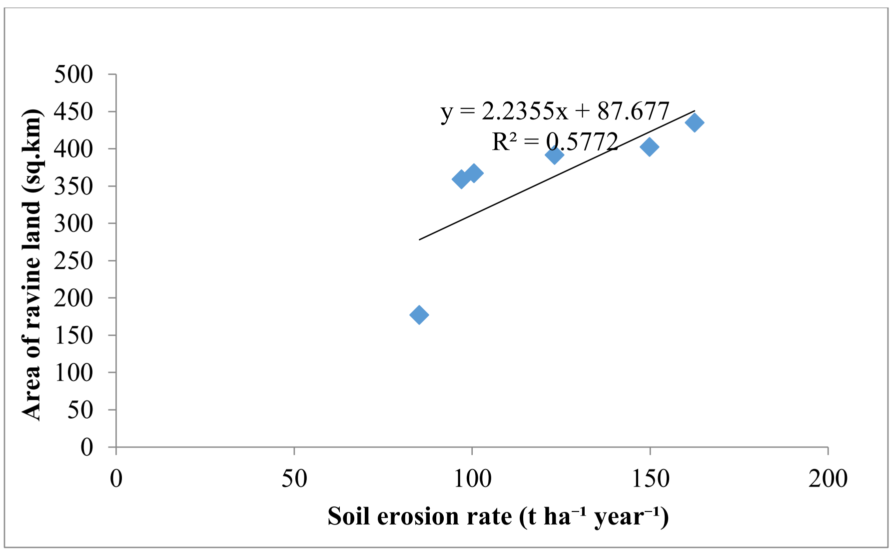

Figure 6: Scatter plot shows a positive relationship between ravine-land area and soil erosion rate, indicating that larger areas of ravine land are generally associated with higher erosion rates

Table 9: Area of ravine land (sq.km) over the years in the study area

Ravine land	1974	1994	2000	2010	2016	2020
Area of ravine land (sq.km)	434.78	391.49	402.38	367.1	359.15	177.07

Article
Journal of Asian Geography, 2026, Volume 5 (Issue 2), 1-17
https://doi.org/10.36777/jag2026.5.2.1
E-ISSN: 2948-5231

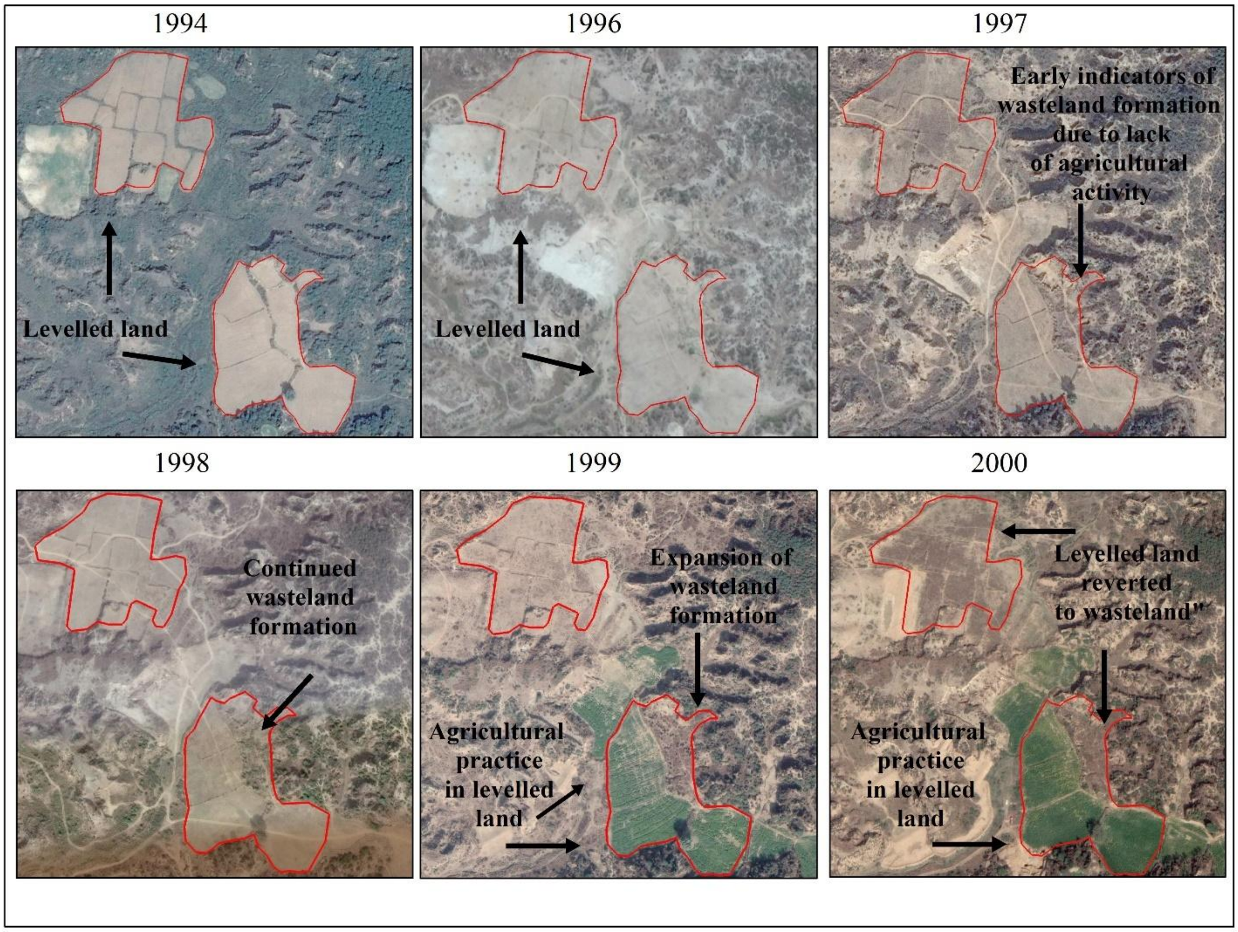

Figure 7: Conversion of ravine levelled land into wasteland due to irregular agricultural practice

Plate 1. Massive land levelling in the study area and conversion of ravine land into agricultural land

Article Journal of Asian Geography, 2026, Volume 5 (Issue 2), 1-17
https://doi.org/10.36777/jag2026.5.2.1
E-ISSN: 2948-5231

5.2 Role of Vegetation Cover in Soil Erosion

In addition to land levelling, vegetation cover was found to play a critical role in mitigating soil erosion over time. Both the Central and State Governments have implemented extensive ecological restoration initiatives in the ravine-affected areas of the study region. Among these, aerial seeding emerged as a key intervention (Khan et al., 2020; Pani, 2016, 2018). In 1980, aerial seeding was implemented in the Bhind district, covering approximately 503 hectares of ravine land (Mudgal, 2005; Pani, 2016; Prasad, 1988; G. Verma et al., 2018). Subsequently, in 1985 and 1993-94, large areas of Chambal ravine land, totaling about 21,063 and 25,000 hectares, respectively, were subjected to aerial seeding (Prasad, 1988). Through aerial seeding, deep ravine zones were planted with vegetation, effectively reducing soil erosion by stabilizing the fragile terrain. Additionally, various protected zones and reserve forests were also introduced in the study area (especially the Etawah district) along the Yamuna River to control soil loss. The National Chambal Sanctuary[1] spans Uttar Pradesh, Madhya Pradesh, and Rajasthan and encompasses approximately 636 sq.km in Uttar Pradesh alone (National Chambal Sanctuary[2]). The Forest Survey of India (FSI) 2021 report also indicated a positive trend in vegetation cover across the study area districts over recent decades, which may have contributed to the reduction in soil erosion rates (Forest Survey of India, 2021; Figure 8a). The increase in vegetation led to many ravine lands being converted into scrubland and plantations, ultimately helping stabilize the soil and minimize erosion rates (Figure 8b).

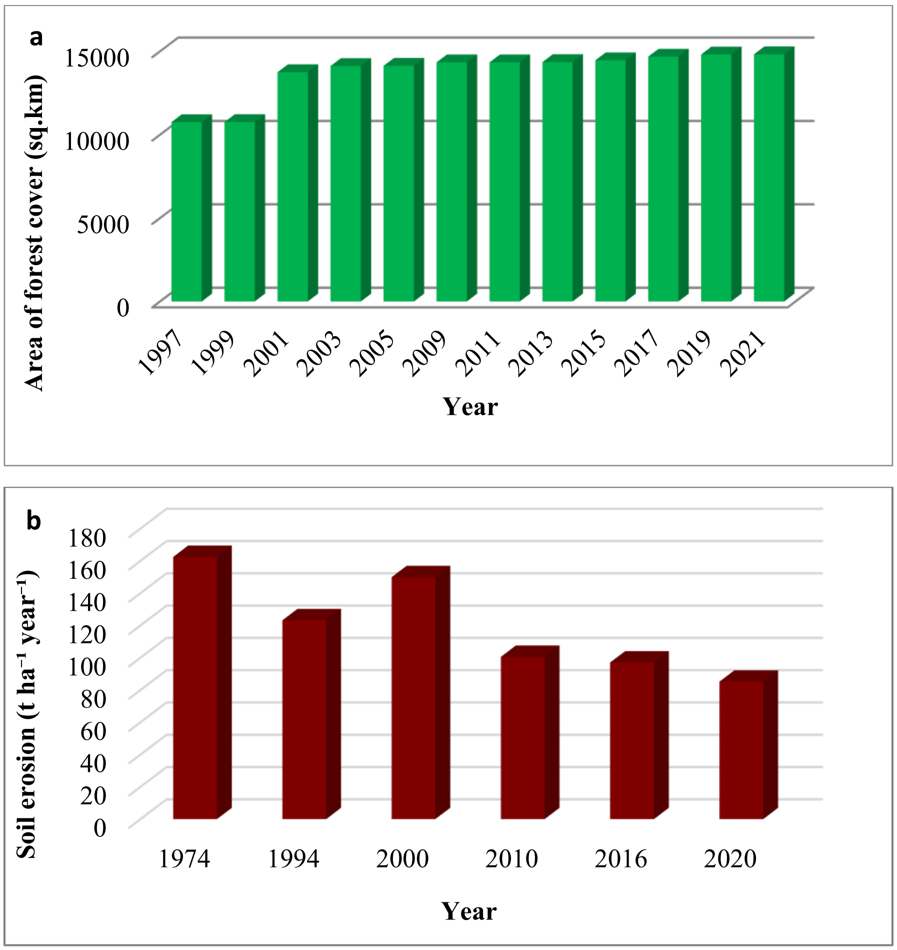

Figure 8: (a) Forest cover in the study-area districts over the years (*Source: Forest Survey of India, 2021*); (b) soil erosion rates over the years

Therefore, the study observed that both ravine land levelling and vegetation growth are effective methods to reduce soil erosion. While ravine land levelling is one approach to protect the land from erosion, the research also noticed that levelled lands may not remain sustainable over the long term without continuous agricultural practices. Hence, continuous agriculture practices on ravine levelled land are also important. If the land is not utilized after levelling, it can start to form small rills and gullies again, eventually turning back into wasteland. Therefore, while land levelling plays a significant role in reducing soil erosion rates, proper utilization and continuous maintenance of levelled ravine land are essential to effectively prevent soil erosion. In contrast, the role of vegetation cover was found to be significant in preventing soil erosion. The study highlights that the introduction of national sanctuaries, protected areas, and increasing trends in vegetation have contributed to the development of substantial dense vegetation cover in the region over the past 20 years. This expansion of vegetation has played a crucial role in reducing soil erosion in this ravine-affected region. While vegetation growth and land levelling have played an important role in reducing surface erosion, gullies in the deeper parts of the ravines continue to grow mainly due to different hydrological processes including headcut migration and fluvial incision (Poesen et al., 2003; Valentin et al., 2005). However, studying these processes was outside the scope of this work.

[1] National Chambal Sanctuary - Wikipedia
[2] National Chambal Sanctuary Uttar Pradesh Eco Tourism | UP Eco-Tourism Development Board | Official Site

E-ISSN: 2948-5231
Article
Journal of Asian Geography, 2026, Volume 5 (Issue 2), 1-17
https://doi.org/10.36777/jag2026.5.2.1

6.0 Validation of the Results

The study evaluated the RUSLE soil erosion map by comparing its spatial distribution with the Bhuvan NRSC land degradation map (2015-16) Figure 9a. The land degradation map clearly delineates areas affected by soil erosion. According to the Bhuvan NRSC data, the study area is classified into different land degradation categories, including sheet erosion, rills, gullies, and shallow and deep ravines. Notably, the map highlights severe deep ravine erosion along the banks of the Yamuna River, resulting in substantial soil loss. Furthermore, it indicates that the area is severely affected by rills and gullies, whereas sheet erosion is less prevalent (Figure 9a). Similarly, the RUSLE model also indicates severe soil erosion along the banks of the Yamuna River (Figure 9b), primarily due to the extensive ravine land. Therefore, the spatial distribution of the RUSLE soil erosion map corresponds well with the Bhuvan NRSC land degradation map. This comparison demonstrates good spatial agreement, indicating that ravine-affected areas correspond to zones of high erosion risk.

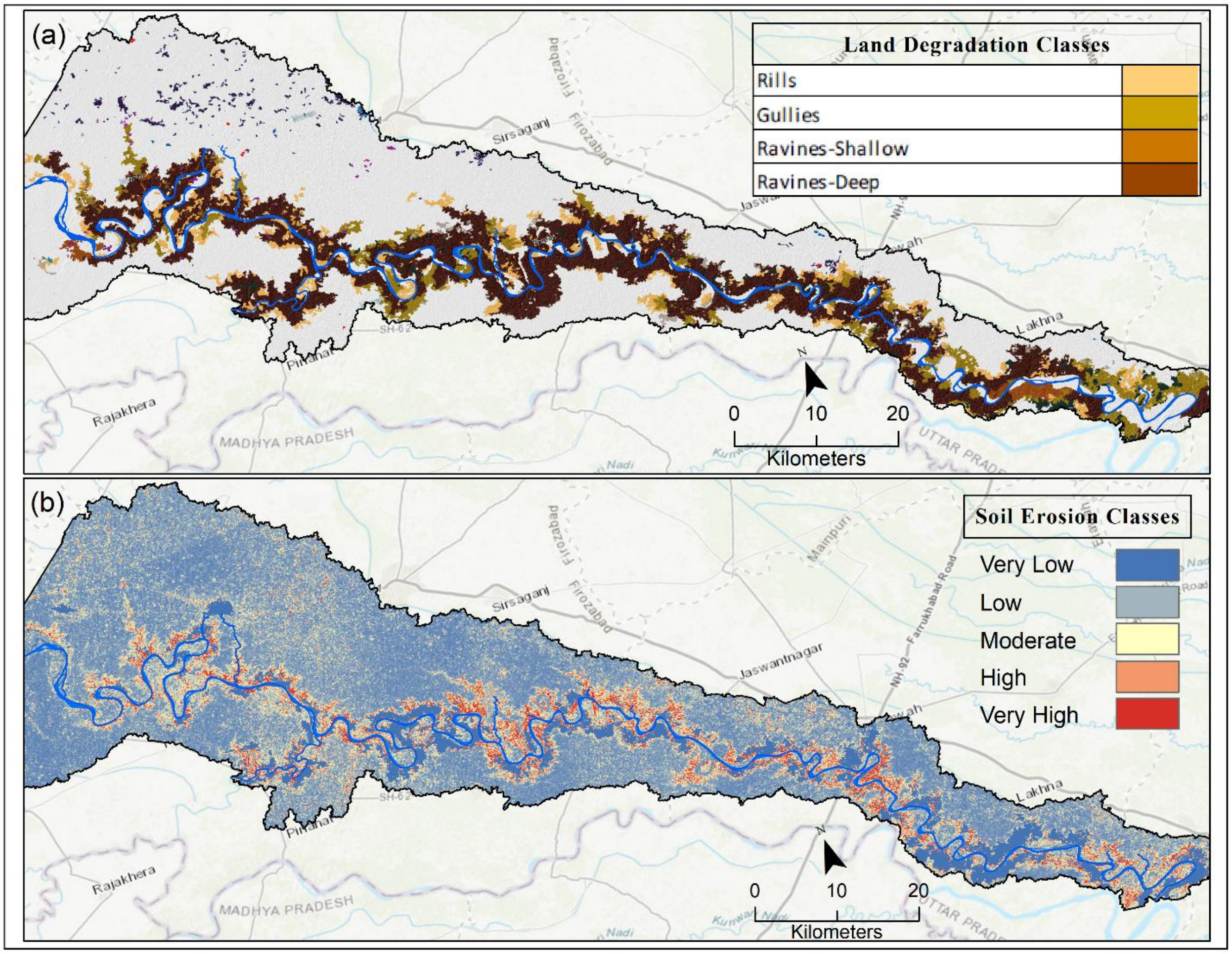

Figure 9: (a) Land degradation map for 2015-16 (*Source: Bhuvan NRSC)*; (b) soil erosion risk map for 2016 generated using the RUSLE model. Both maps indicate higher soil loss along the banks of the Yamuna River.

7.0 Limitations

Although the RUSLE model is widely used tool for estimating soil erosion rates and mapping their spatial distribution, it has several inherent limitations. RUSLE is an empirical model designed to estimate long-term annual average soil loss caused by sheet and rill erosion during rainfall events (Renard et al., 1997). Therefore, it provides an estimate of potential soil erosion risk rather than actual sediment yield and does not explicitly account for sediment losses associated with gully erosion. Consequently, the model outputs presented in this study represent potential soil erosion risk and do not include the total sediment losses resulting from gully erosion processes. Actual sediment losses in gully-dominated landscapes, such as ravine regions, may therefore be higher than the estimates reported here. Despite these limitations, the primary objective of the present study was to estimate potential soil loss per unit area and identify the spatial distribution of areas at high risk of soil erosion, rather than to model gully initiation or characterise gully dynamics. In this context, the RUSLE model has been widely recognised and successfully applied to assess potential soil erosion in diverse landscapes, including complex ravine- and gully-affected regions (Kebede et al., 2021; Kumar et al., 2022; Mohapatra, 2022; Tang et al., 2015). Therefore, the model is considered appropriate for achieving the objectives of the present study. This research also provides a baseline assessment of the application of the RUSLE model in highly dissected ravine landscapes and demonstrates a methodological framework that may be applicable to other ravine-prone regions experiencing similar soil degradation problems.

All factors used in the RUSLE model were derived using methodologies widely adopted in regional-scale soil erosion studies. The consistent use of these methodologies and data sources across all study periods provides a reliable basis for evaluating the spatial and temporal patterns of soil erosion. Nevertheless, uncertainties may remain associated with several model input factors. For example, the R-factor was estimated using an empirical rainfall erosivity equation (**Eq.2**) because rainfall intensity and storm kinetic energy data were unavailable for the study area. Similarly, the C-factor was derived from satellite-based NDVI (Eq.5), whereas P-factor values were assigned from published literature according to land-use classes (Table 3). In addition, satellite images with different spatial resolutions (10-80 m) were resampled to a common 30 m spatial resolution to maintain consistency among the RUSLE input factors. Although this approach is widely adopted in multi-temporal remote sensing studies, resampling may introduce minor uncertainties in NDVI estimation and, consequently, in the derived C-factor values (Jiang et al., 2006; Leeuwen et al., 2006). Therefore, these factors may introduce some uncertainty into the absolute values of the estimated soil erosion rates. However, because of the same methodologies, datasets, and processing procedures were consistently applied throughout the study period, they provide a robust basis for evaluating the relative spatial and temporal patterns of soil erosion across the study area.

Another important limitation concerns the validation of the model results. Although the spatial distribution of the estimated soil erosion was evaluated using the Bhuvan NRSC land degradation map and showed good spatial agreement with the observed erosion-prone areas (**Fig.9a**), the dataset does not provide quantitative measurements of soil loss or sediment yield. Furthermore, long-term field observations, and sediment yield data were unavailable for the study area during the study period. Consequently, the absolute magnitude of the predicted soil loss values could not be quantitatively validated. Nevertheless, the model remains suitable for identifying erosion-prone areas and evaluating their relative spatial and temporal variations. Future studies should integrate field measurements and sediment monitoring to improve the quantitative validation of RUSLE-based soil erosion estimates and to provide a better understanding of gully erosion processes.

8.0 Conclusions

The findings of this research underscore the critical importance of addressing soil erosion, a significant global issue with significant environmental and socio-economic implications. As countries try to achieve Sustainable Development Goals (SDGs), particularly those related to land degradation neutrality, climate action, and food security, the prevention of soil erosion must be prioritized on the policy and research agenda. There is a need for concerted efforts among researchers, scientists, and policymakers to mitigate erosion risks and safeguard soil resources. This study focused on estimating field soil erosion in a ravine-affected area along the banks of the Yamuna River, employing the Revised Universal Soil Loss Equation (RUSLE) model with various erosion estimation parameters. The results revealed that high soil erosion rates are mainly associated with the ravine-affected areas, due to the highly dissected nature of the ravine land, which facilitates increased soil loss. Previous studies (Khan & Govil, 2020; Mohapatra, 2022) have also identified the highest soil erosion rates in the ravine and steeply sloping areas. Although the estimated erosion magnitude differs among studies due to differences in study extent, spatial resolution, and datasets, the overall spatial erosion pattern observed in the present study is consistent with previous findings. However, amidst these challenges, the research also identified promising trends, indicating a decline in soil erosion rates over time. This decline correlated with interventions such as land levelling and ravine land conversion, which reduced the extent of ravine land and promoted vegetation cover. Although the research also observed the importance of continuous agriculture practice in the ravine levelled land, otherwise, the land starts forming small rills and gullies, eventually turning back into wasteland. Therefore, land levelling is one way to prevent ravine erosion, but continuous agriculture or vegetation cover is much more important to prevent ravine erosion. These findings highlight the potential of improved land management practices to mitigate soil erosion even in highly vulnerable areas. By implementing effective conservation measures, such as contour farming, terracing, and afforestation, it is possible to enhance soil stability and reduce erosion risk. Additionally, sustainable land practices, coupled with community engagement and policy support, can contribute to long-term erosion prevention and ecosystem resilience.

In conclusion, this study emphasizes that through improved land management practices, restoration efforts, and sustainable practices, it is possible to protect land from further erosion. Based on the results presented and the observed trend of soil erosion rates, the study concludes that implementing better land practices can effectively reduce the rate of soil erosion, even in ravine-affected areas prone to severe degradation.

Acknowledgement: This study forms part of the first author's M.Phil. thesis, carried out at the Centre for the Study of Regional Development (CSRD), Jawaharlal Nehru University (JNU), New Delhi.

Conflicts of Interest: The authors declare no conflict of interest in this study

Data Availability: The data used in the study is available in the public domain. Cartosat DEM data is available at https://bhuvan.nrsc.gov.in/home/. Precipitation data is available at https://indiawris.gov.in/. Soil textural data is available at https://www.fao.org/. Satellite datasets were taken from https://earthexplorer.usgs.gov/ and https://scihub.copernicus.eu/.

Ethical approval: As the study is based on secondary data available in the public domain for research, no ethical approval was required from any institutional review board (IRB).

Funding: The authors received no financial support for this research. The research was conducted solely for academic purposes.

Author contributions: Both authors contributed equally to each section of the study and have read and approved of the final manuscript.

References

Almagro, A., Thomé, T. C., Colman, C. B., Pereira, R. B., Marcato Junior, J., Rodrigues, D. B. B., & Oliveira, P. T. S. (2019). Improving cover and management factor (C-factor) estimation using remote sensing approaches for tropical regions. International Soil and Water Conservation Research, 7(4), 325–334. https://doi.org/10.1016/j.iswcr.2019.08.005

Benavidez, R., Jackson, B., Maxwell, D., & Norton, K. (2018). A review of the (Revised) Universal Soil Loss Equation ((R)USLE): With a view to increasing its global applicability and improving soil loss estimates. Hydrology and Earth System Sciences, 22(11), 6059–6086. https://doi.org/10.5194/hess-22-6059-2018

Biswas, S., & Pani, P. (2015). Estimation of soil erosion using RUSLE and GIS techniques: A case study of Barakar River basin, Jharkhand, India. Modeling Earth Systems and Environment, 1(4). https://doi.org/10.1007/s40808-015-0040-3

Boardman, J. (2014). How old are the gullies (dongas) of the Sneeuberg uplands, Eastern Karoo, South Africa? Catena, 113, 79–85. https://doi.org/10.1016/j.catena.2013.09.012

Borrelli, P., Robinson, D. A., Fleischer, L. R., Lugato, E., Ballabio, C., Alewell, C., Meusburger, K., Modugno, S., Schütt, B., Ferro, V., Bagarello, V., Van Oost, K., Montanarella, L., & Panagos, P. (2017). An assessment of the global impact of 21st century land use change on soil erosion. Nature Communications, 8, Article 2013. https://doi.org/10.1038/s41467-017-02142-7

Chadli, K. (2016). Estimation of soil loss using RUSLE model for Sebou watershed (Morocco). Modeling Earth Systems and Environment, 2(2). https://doi.org/10.1007/s40808-016-0105-y

E-ISSN: 2948-5231
Article
Journal of Asian Geography, 2026, Volume 5 (Issue 2), 1-17
https://doi.org/10.36777/jag2026.5.2.1

Chatterjee, R. S., Saha, S. K., Kumar, S., Mathew, S., Lakhera, R. C., & Dadhwal, V. K. (2009). Interferometric SAR for characterization of ravines as a function of their density, depth, and surface cover. ISPRS Journal of Photogrammetry and Remote Sensing, 64(5), 472–481. https://doi.org/10.1016/j.isprsjprs.2008.12.005

Chatterjee, S., Krishna, A. P., & Sharma, A. P. (2014). Geospatial assessment of soil erosion vulnerability at watershed level in some sections of the Upper Subarnarekha River basin, Jharkhand, India. Environmental Earth Sciences, 71(1), 357–374. https://doi.org/10.1007/s12665-013-2439-3

Chuenchum, P., Xu, M., & Tang, W. (2020). Estimation of soil erosion and sediment yield in the Lancang-Mekong River using the modified revised universal soil loss equation and GIS techniques. Water, 12(1), Article 135. https://doi.org/10.3390/w12010135

Colman, C. B. (2018). Impacts of climate and land use changes on soil erosion in the Upper Paraguay Basin. Universidade Federal de Mato Grosso do Sul.

de Vente, J., & Poesen, J. (2005). Predicting soil erosion and sediment yield at the basin scale: Scale issues and semi-quantitative models. Earth-Science Reviews, 71(1–2), 95–125. https://doi.org/10.1016/j.earscirev.2005.02.002

Desmet, P. J. J., & Govers, G. (1996). A GIS procedure for automatically calculating the USLE LS factor on topographically complex landscape units. Journal of Soil and Water Conservation, 51(5), 427–433. https://doi.org/10.1080/00224561.1996.12457102

Durigon, V. L., Carvalho, D. F., Antunes, M. A. H., Oliveira, P. T. S., & Fernandes, M. M. (2014). NDVI time series for monitoring RUSLE cover management factor in a tropical watershed. International Journal of Remote Sensing, 35(2), 441–453. https://doi.org/10.1080/01431161.2013.871081

Ebrahimzadeh, S., Motagh, M., Mahboub, V., & Mirdar Harijani, F. (2018). An improved RUSLE/SDR model for the evaluation of soil erosion. Environmental Earth Sciences, 77(12), Article 454. https://doi.org/10.1007/s12665-018-7635-8

Eslamian, S. (Ed.). (2014). Handbook of engineering hydrology: Modeling, climate change and variability. CRC Press.

Food and Agriculture Organization of the United Nations, & Intergovernmental Technical Panel on Soils. (2015). Status of the world's soil resources. Food and Agriculture Organization of the United Nations.

Forest Survey of India. (2021). India state of forest report 2021.

Grauso, S., Verrubbi, V., Zini, A., Peloso, A., Crovato, C., & Sciortino, M. (2015). Soil erosion estimate in southern Latium (Central Italy) using RUSLE and geostatistical techniques (ENEA Technical Report RT/2015/22). ENEA. https://iris.enea.it/handle/20.500.12079/6719

Gupta, S. (2015). Simulating climate change impact on soil erosion & soil carbon sequestration [Master's thesis, Indian Institute of Remote Sensing]. Indian Institute of Remote Sensing.

Hajgh, M. J. (1984). Ravine erosion and reclamation in India. GeoForum, 15(4), 543–561. https://doi.org/10.1016/0016-7185(84)90024-1

Huffman, R. L., Fangmeier, D. D., Elliot, W. J., & Workman, S. R. (2013). Soil and water conservation engineering (7th ed.). American Society of Agricultural and Biological Engineers. https://doi.org/10.13031/swce.2013

Jiang, Z., Huete, A. R., Chen, J., Chen, Y., Li, J., Yan, G., & Zhang, X. (2006). Analysis of NDVI and scaled difference vegetation index retrievals of vegetation fraction. Remote Sensing of Environment, 101(3), 366–378. https://doi.org/10.1016/j.rse.2006.01.003

Kabanza, A. K., Dondeyne, S., Kimaro, D. N., Kafiriti, E., & Poesen, J. (2013). Effectiveness of soil conservation measures in two contrasting landscape units of southeastern Tanzania. Zeitschrift für Geomorphologie, 57, 269–288. https://doi.org/10.1127/0372-8854/2013/0102

Kebede, Y. S., Endalamaw, N. T., Sinshaw, B. G., & Atinkut, H. B. (2021). Modeling soil erosion using RUSLE and GIS at watershed level in the Upper Beles, Ethiopia. Environmental Challenges, 2, Article 100009. https://doi.org/10.1016/j.envc.2020.100009

Khan, A., & Govil, H. (2020). Evaluation of potential sites for soil erosion risk in and around Yamuna River flood plain using RUSLE. Arabian Journal of Geosciences, 13(15). https://doi.org/10.1007/s12517-020-05646-7

Khan, A., Govil, H., Kumar, G., & Dave, R. (2020). Synergistic use of Sentinel-1 and Sentinel-2 for improved LULC mapping with special reference to bad land class: A case study for Yamuna River floodplain, India. Spatial Information Research, 28(6), 669–681. https://doi.org/10.1007/s41324-020-00325-x

Knijff, J. M. van der, Jones, R. J. A., & Montanarella, L. (2000). Soil erosion risk assessment in Europe. European Soil Bureau, European Commission.

Kumar, R., Deshmukh, B., & Kumar, A. (2022). Using Google Earth Engine and GIS for basin-scale soil erosion risk assessment: A case study of Chambal River basin, central India. Journal of Earth System Science, 131(4), Article 228. https://doi.org/10.1007/s12040-022-01977-z

Lakkad, A., & Shrivastava, P. K. (2016). Estimation of cover management factor of RUSLE at sub-watershed level. AGRES – An International e-Journal, 5(4), 406–412.

Lal, R. (2003). Soil erosion and the global carbon budget. Environment International, 29(4), 437–450. https://doi.org/10.1016/S0160-4120(02)00192-7

Lane, L. J., Renard, K. G., Foster, G. R., & Laflen, J. M. (1992). Development and application of modern soil erosion prediction technology: The USDA experience. Soil and Water Management and Conservation, 30, 893–912.

van Leeuwen, W. J. D., Orr, B. J., Marsh, S. E., & Herrmann, S. M. (2006). Multi-sensor NDVI data continuity: Uncertainties and implications for vegetation monitoring applications. Remote Sensing of Environment, 100(1), 67–81. https://doi.org/10.1016/j.rse.2005.10.002

Manivannan, S., Thilagam, V. K., & Khola, O. P. S. (2017). Soil and water conservation in India: Strategies and research challenges. Journal of Soil and Water Conservation, 16(4), 312. https://doi.org/10.5958/2455-7145.2017.00046.7

Marzolff, I., & Pani, P. (2018). Dynamics and patterns of land levelling for agricultural reclamation of erosional badlands in Chambal Valley (Madhya Pradesh, India). Earth Surface Processes and Landforms, 43(2), 524–542. https://doi.org/10.1002/esp.4266

Miheretu, B. A., & Yimer, A. A. (2018). Estimating soil loss for sustainable land management planning at the Gelana sub-watershed, northern highlands of Ethiopia. International Journal of River Basin Management, 16(1), 41–50. https://doi.org/10.1080/15715124.2017.1351978

Mohapatra, R. (2022). Application of revised universal soil loss equation model for assessment of soil erosion and prioritization of ravine-infested sub-basins of a semi-arid river system in India. Modeling Earth Systems and Environment, 8(4), 4883–4896. https://doi.org/10.1007/s40808-022-01388-5

Montgomery, D. R. (2007). Soil erosion and agricultural sustainability. Proceedings of the National Academy of Sciences, 104(33), 13268–13272. https://doi.org/10.1073/pnas.0611508104

Morgan, R. P. C., Quinton, J. N., Smith, R. E., Govers, G., Poesen, J. W. A., Auerswald, K., Chisci, G., Torri, D., & Styczen, M. E. (1998). The European soil erosion model (EUROSEM): A dynamic approach for predicting sediment transport from fields and small catchments. Earth Surface Processes and Landforms, 23(6), 527–544. https://doi.org/10.1002/(SICI)1096-9837(199806)23:6<527::AID-ESP868>3.0.CO;2-5

Mudgal, M. K. (2005). Socio-economic impact of ravine lands: A case study of River Chambal basin of state of Madhya Pradesh, India. Geophysical Research Abstracts, 7, 1–6.

Nadal-Romero, E., & Regüés, D. (2010). Geomorphological dynamics of subhumid mountain badland areas: Weathering, hydrological and suspended sediment transport processes: A case study in the Araguás catchment (Central Pyrenees) and implications for altered hydroclimatic regimes. Progress in Physical Geography, 34(2), 123–150. https://doi.org/10.1177/0309133309356624
Narayana, D. V. V., & Babu, R. (1983). Estimation of soil erosion in India. Journal of Irrigation and Drainage Engineering, 109(4), 419–434. https://doi.org/10.1061/(ASCE)0733-9437(1983)109:4(419)
Nearing, M. A., Xie, Y., Liu, B., Ye, Y., & Bennett, H. H. (2017). Natural and anthropogenic rates of soil erosion. International Soil and Water Conservation Research, 5(2), 77–84. https://doi.org/10.1016/j.iswcr.2017.04.001
Oldeman, L. R. (2000). Impact of soil degradation: A global scenario (ISRIC Report 2000/01). International Soil Reference and Information Centre.
Pak, J., Fleming, M., Scharffenberg, W., & Ely, P. (2008). Soil erosion and sediment yield modeling with the Hydrologic Modeling System (HEC-HMS). In World Environmental and Water Resources Congress 2008: Ahupua'a (pp. 316–?). https://doi.org/10.1061/40976(316)362
Pal, S. (2016). Identification of soil erosion vulnerable areas in Chandrabhaga River basin: A multi-criteria decision approach. Modeling Earth Systems and Environment, 2(1), 1–11. https://doi.org/10.1007/s40808-015-0052-z
Pandey, A., Chowdary, V. M., & Mal, B. C. (2007). Identification of critical erosion prone areas in the small agricultural watershed using USLE, GIS and remote sensing. Water Resources Management, 21(4), 729–746. https://doi.org/10.1007/s11269-006-9061-z
Pani, P. (2016). Controlling gully erosion: An analysis of land reclamation processes in Chambal Valley, India. Development in Practice, 26(8), 1047–1059. https://doi.org/10.1080/09614524.2016.1228831
Pani, P. (2018). Ravine erosion and livelihoods in semi-arid India: Implications for socioeconomic development. Journal of Asian and African Studies, 53(3), 437–454. https://doi.org/10.1177/0021909616689798
Pani, P. (2020). Land degradation and socio-economic development: A field-based perspective. Springer. https://doi.org/10.1007/978-3-030-42074-1
Pani, P., & Mohapatra, S. N. (2011). Ravine erosion in India. Geography and You, (68).
Pani, P., Routh, R., & Mohapatra, S. N. (2022). Assessment of soil erosion and sediment yield in a semi-arid region of India using RUSLE and geospatial techniques. Annals of the National Association of Geographers India, 42(2), 22–44.
Pimentel, D., Harvey, C., Resosudarmo, P., Sinclair, K., Kurz, D., McNair, M., Crist, S., Shpritz, L., Fitton, L., Saffouri, R., & Blair, R. (1995). Environmental and economic costs of soil erosion and conservation benefits. Science, 267(5201), 1117–1123. https://doi.org/10.1126/science.267.5201.1117
Poesen, J., Nachtergaele, J., Verstraeten, G., & Valentin, C. (2003). Gully erosion and environmental change: Importance and research needs. Catena, 50(2–4), 91–133. https://doi.org/10.1016/S0341-8162(02)00143-1
Prasad, R. (1988). Effectiveness of aerial seeding in reclamation of Chambal ravines in Madhya Pradesh. Indian Forester, 114(1), 1–18. https://doi.org/10.36808/if/1988/v114i1/9161
Prasannakumar, V., Vijith, H., Abinod, S., & Geetha, N. (2012). Estimation of soil erosion risk within a small mountainous sub-watershed in Kerala, India, using Revised Universal Soil Loss Equation (RUSLE) and geo-information technology. Geoscience Frontiers, 3(2), 209–215. https://doi.org/10.1016/j.gsf.2011.11.003
Ranga, V., Poesen, J., van Rompaey, A., Mohapatra, S. N., & Pani, P. (2016). Detection and analysis of badlands dynamics in the Chambal River Valley (India), during the last 40 (1971–2010) years. Environmental Earth Sciences, 75(3), Article 183. https://doi.org/10.1007/s12665-015-5017-z
Rejani, R., Rao, K. V., Osman, M., Srinivasa Rao, C., Reddy, K. S., Chary, G. R., Pushpanjali, & Samuel, J. (2016). Spatial and temporal estimation of soil loss for the sustainable management of a wet semi-arid watershed cluster. Environmental Monitoring and Assessment, 188(3), Article 178. https://doi.org/10.1007/s10661-016-5143-4
Renard, K. G., Foster, G. R., Weesies, G. A., McCool, D. K., & Yoder, D. C. (1997). Predicting soil erosion by water: A guide to conservation planning with the Revised Universal Soil Loss Equation (RUSLE) (Agriculture Handbook No. 703). U.S. Department of Agriculture, Agricultural Research Service.
Renschler, C. S., & Harbor, J. (2002). Soil erosion assessment tools from point to regional scales: The role of geomorphologists in land management research and implementation. Geomorphology, 47(2–4), 189–209. https://doi.org/10.1016/S0169-555X(02)00082-X
Roy, P. (2019). Application of USLE in a GIS environment to estimate soil erosion in the Irga watershed, Jharkhand, India. Physical Geography, 1–23. https://doi.org/10.1080/02723646.2018.1550301
Sharma, H. S. (Ed.). (1982). Perspectives in geomorphology: Applied geomorphology (Vol. 3). Concept Publishing.
Sikka, A. K., Mishra, P. K., Singh, R. K., Rao, B. K., & Islam, A. (2018). Technological interventions for managing ravine lands for livelihood and environmental security. In Ravine lands: Greening for livelihood and environmental security (pp. 217–236). Springer. https://doi.org/10.1007/978-981-10-8043-2_9
Singh, G., Babu, R., & Chandra, S. (1981). Soil loss prediction research in India. Central Soil and Water Conservation Research and Training Institute.
Smith, H. J. (1999). Application of empirical soil loss models in southern Africa: A review. South African Journal of Plant and Soil, 16(3), 158–163. https://doi.org/10.1080/02571862.1999.10635003
Sonderegger, T., & Stephan, P. (2021). Global assessment of agricultural productivity losses from soil compaction and water erosion. Environmental Science & Technology, 55(18), 12162–12171. https://doi.org/10.1021/acs.est.1c03774
Tagore, G. S., Bairagi, G. D., Sharma, R., Porte, S. S., & Vishwakarma, M. (2021). Appraisal of spatial distribution of degraded lands using geo-spatial techniques. Communications in Soil Science and Plant Analysis, 52(6), 601–612. https://doi.org/10.1080/00103624.2020.1862159
Tang, Q., Xu, Y., Bennett, S. J., & Li, Y. (2015). Assessment of soil erosion using RUSLE and GIS: A case study of the Yangou watershed in the Loess Plateau, China. Environmental Earth Sciences, 73(4), 1715–1724. https://doi.org/10.1007/s12665-014-3523-z
Tosic, R., Dragicevic, S., Kostadinov, S., & Dragovic, N. (2011). Assessment of soil erosion potential by the USLE method: Case study, Republic of Srpska–BiH. Fresenius Environmental Bulletin, 20(8), 1910–1917.
Valentin, C., Poesen, J., & Li, Y. (2005). Gully erosion: Impacts, factors and control. Catena, 63(2–3), 132–153. https://doi.org/10.1016/j.catena.2005.06.001
van Rompaey, A. J. J., Govers, G., & Puttemans, C. (2002). Modelling land use changes and their impacts on soil erosion and sediment supply to rivers. Earth Surface Processes and Landforms, 27(5), 481–494. https://doi.org/10.1002/esp.335
Verma, G., Singh, Y. P., Singh, A. K., & Verma, S. (2018). Management of Chambal ravines for income enhancement. In Ravine lands: Greening for livelihood and environmental security. Springer. https://doi.org/10.1007/978-981-10-8043-2
Verma, S. K., Singh, A. K., Singh, A., & Prasad, J. (2021). Greening of Chambal ravine: Site-specific approach for sustainable development.

E-ISSN: 2948-5231
Article
Journal of Asian Geography, 2026, Volume 5 (Issue 2), 1-17
https://doi.org/10.36777/jag2026.5.2.1

Journal of Soil and Water Conservation, 20(4), 375–385. https://doi.org/10.5958/2455-7145.2021.00047.3
Vinay, M., & Mahalingam, B. (2015). Quantification of soil erosion by water using GIS and remote sensing techniques: A study of Pandavapura Taluk, Mandya District, Karnataka, India. ARPN Journal of Earth Sciences, 4(2), 103–110.
Vrieling, A. (2006). Satellite remote sensing for water erosion assessment: A review. Catena, 65(1), 2–18. https://doi.org/10.1016/j.catena.2005.10.005
Wischmeier, W. H., & Smith, D. D. (1978). Predicting rainfall erosion losses: A guide to conservation planning (Agriculture Handbook No. 537). U.S. Department of Agriculture.
Woodroffe, C. D., Jones, B. G., & Simms, A. D. (2003). Application of RUSLE for erosion management in a coastal catchment, southern NSW. In MODSIM 2003: International Congress on Modelling and Simulation: Integrative modelling of biophysical, social and economic systems for resource management solutions (Vol. 2, pp. 678–683). Modelling and Simulation Society of Australia and New Zealand.
Woodward, D. E. (1999). Method to predict cropland ephemeral gully erosion. Catena, 37(3–4), 393–399. https://doi.org/10.1016/S0341-8162(99)00028-4